



## Letter to the Editor

## Ferromagnetic shape memory flapper

## ARTICLE INFO

## Keywords:

Ferromagnetic shape memory alloys  
Propulsion

## ABSTRACT

A new method for propulsion using a  $Ni_2MnGa$  ferromagnetic shape memory flapper is introduced. We optically examine the magnetic field induced strain of pure shear by means of a state of the art generator that provides alternating magnetic fields of 7000 Oe at frequencies of up to 100 Hz. Preliminary measurements show local shear deformation of about 5%, which open new frontiers in propulsion mechanisms.

© 2009 Elsevier B.V. All rights reserved.

Flapping mechanisms that generate propulsion for swimming and flying are abundant in nature. One way of obtaining motion is by a transverse movement of surfaces in media which forms lateral thrust, thus propelling the body. Of a great interest are systems that can produce propulsion at scales of millimeter down to a micron, or perhaps smaller. Possible candidates for those tasks are active materials. These materials are commonly applied as actuation devices in Micro Electro Mechanical Systems (MEMS) [1,2]. Nowadays, self-propelled methods for micro-robots applications are being developed. For example, a swimming micro-robot in the body which creates a traveling wave in an elastic tail made of piezoelectric actuators [3]. However, piezoelectric materials as well as magnetostrictive materials are limited to very small strains, and therefore different active materials are needed.

Among active materials, shape memory alloys offer the largest work output per cycle accompanied by huge strains [4]. Temperature change induces a structural transformation from austenitic to martensitic phase, thus producing large strains. These materials are attractive for MEMS applications, but for the problem of small-scale autonomous motion, the difficulty of supplying temperature pulses to a moving vehicle seems hard to overcome [5]. Moreover, the ability to generate high gradients of temperature for this motion is limited by the heat conduction of the alloy and its surroundings. In recent years, a sub class of shape memory alloys known as ferromagnetic shape memory [6] (FSM) alloys has received much attention because they can provide large strains and have fast responses to external magnetic fields [7]. Unlike temperature controlled shape memory actuation, the ferromagnetic shape memory actuation can also be induced by fast rearrangement of twin variants of the martensite. By applying a magnetic field to the martensitic state, they can be made to undergo large deformations, comparable to that produced by the best shape memory materials.

The problem being considered here is only part of the larger problem of, how does one produce motion through a fluid. From the scaling laws of the Navier-Stokes equations of fluid mechanics, viscous forces are greatly exaggerated at small scales. Thus the forces required to overcome viscous forces at small scales are enormous. For such applications actuators that have large work output per unit volume are desired. At first, a cantilever seems to be a particularly

unfavorable choice for a small scale actuator from a structural perspective. That is, a bent cantilever of thickness  $h$  stores (or produces) energy that scales as  $h^3$ . This follows for classical elastic beams from Euler-Bernoulli theory, but it is a much more general result [8]. Milliaactuators have been built [4] with actuation produced by bilayers of NiTi shape memory alloy and Si that work in bending. These show work output far less than expected based on the theoretical values exactly because of the prefactor  $h^3$ . However, shape memory, and ferromagnetic shape memory materials have exceedingly low shear stiffness for certain modes of shear. Thus, designed properly, a ferromagnetic shape memory beam can be made to “bend” using an applied field by the mechanism of shear deformation, and produce work output proportional to  $h$  [9]. In this paper, the first steps of this type of motion is introduced, in which we demonstrate the magnetic field induced strain of  $Ni_2MnGa$  FSM alloy, where the shearing mechanism is directly produced by twin boundary motion.

A typical martensitic microstructure of  $Ni_2MnGa$  consists of mixtures of three tetragonal variants, in which two adjacent variants meet at well-defined twin boundaries [6]. On the one hand, such patterns satisfy the mechanical compatibility condition between tetragonal variants. On the other hand they comply with the magnetic boundary continuity conditions on variant planes on both sides of a twin boundary. Such compatibility coupling between the elastic and magnetic subsystems occurs due to the coincidence of the  $c$ -axis of the tetragonal lattice distortions with the directions of easy magnetization. Since the magnetization only assumes two possible directions, an external magnetic field  $H$  that favors alternately between these two will align the magnetization towards the field, resulting in variant rearrangement.

Proper orientation of twin boundaries in the  $Ni_2MnGa$  FSM alloy can lead to the desirable shear. To do so, the sample should be practically cut to the new orientation. The induced strain tensor in the new cut orientation  $E'$  can be obtained by calculating  $E' = Q^T E Q$ , where  $Q$  is the cosine direction matrix that rotate the original global axis to the new orientation. The strain tensor  $E$  is derived from the specimen that produces extensional strain with twin boundaries oriented at  $45^\circ$ . Calculating  $E'$  shows that a specimen cut along the  $[1\ 1\ 0]$  orientation can yield pure shear strain of about 6% [10]. Therefore, the assignment of a magnetic fields in the  $[1\ 0\ 0]$  and

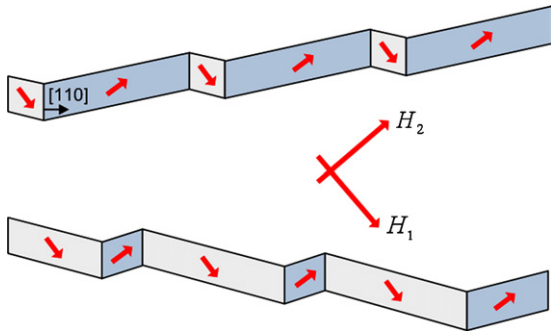


Fig. 1. Illustration of the expected shear motion of the flapper.

[0 1 0] directions to specimens cut along the [1 1 0] orientation, as illustrated in Fig. 1, is expected to alternately favor between these two variants to produce a flapping motion.

A unique Alternating Magnetic Field Generator (AMFG) [7] was developed to provide alternating magnetic fields at frequencies of up to 100 Hz and to obtain the desired actuation, as illustrated in Fig. 2a. The instrument was designed to generate two alternat-

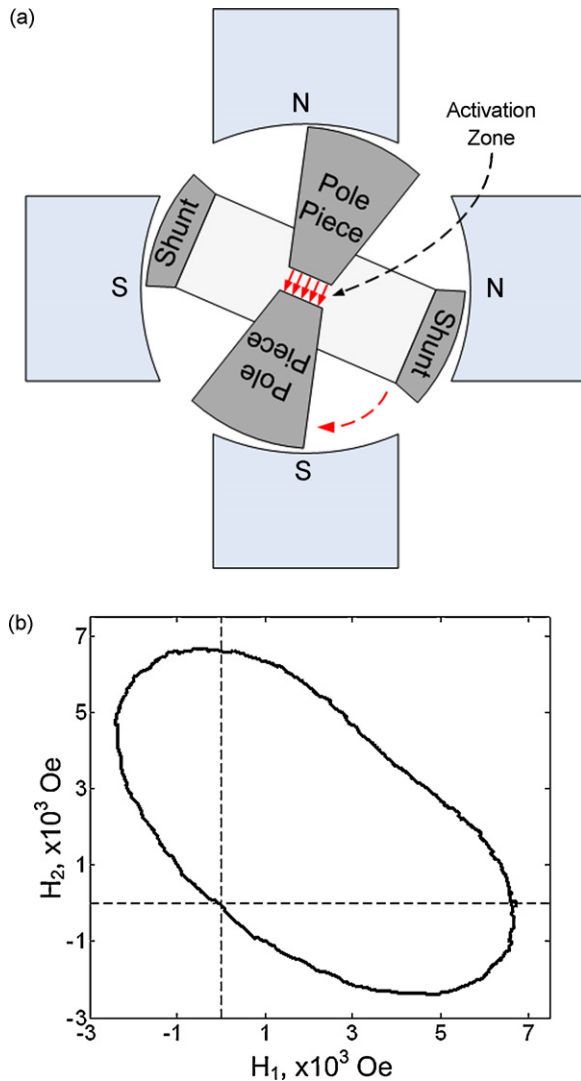


Fig. 2. (a) Illustration of the Alternating Magnetic Field Generator (AMFG). (b) Measured magnetic field  $H_2$  as a function of the perpendicular magnetic field  $H_1$ , generated by the AMFG.

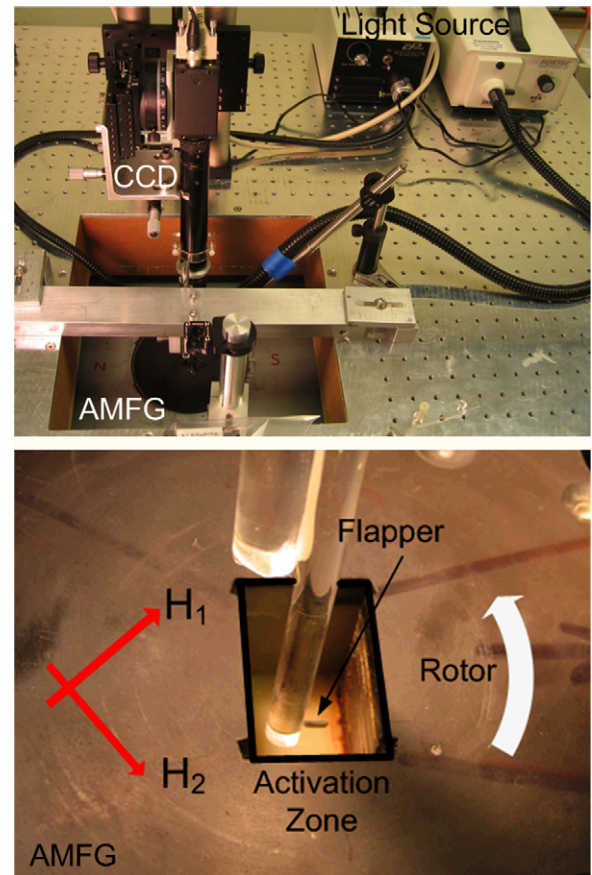
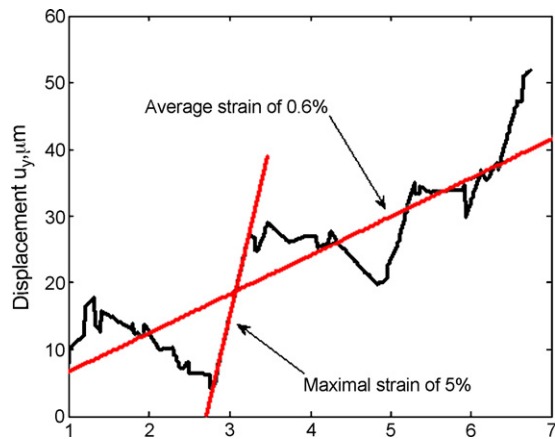


Fig. 3. Photograph of the experimental apparatus. (a) The AMFG, light sources, CCD camera and specimen holder (b) zoom in on the flapper, located at the center of the activation zone of the AMFG.

ing orthogonal magnetic fields as needed for the variant switching experiment. That field structure is important both to minimize nucleation of  $180^\circ$  magnetization domains which cause energy loss without strain production, and to provide two-way actuation. The generator comprises of two perpendicular pairs of permanent magnets, and a rotor which contains a pair of pole pieces and a field shunt. When the pole pieces are located between one pair of magnets, they channel the magnetic field to the air gap, referred to as the activation zone. At the same time the shunt prevents the magnetic field of the second pair of magnets from generating magnetic field in the activation zone by providing a magnetic circuit around the activation zone. After a  $90^\circ$  rotation the role of the magnets is swapped, and thus the alternating magnetic field is generated. The driving magnetic field distribution of the AMFG was measured using a gauss-meter (Lakeshore Inc., 475 DSP) in two perpendicular directions  $H_1$ - $H_2$  with a transverse Hall probe (Lakeshore Inc., HMMT-6J08-VR). The magnetic field variation over a cycle is shown in Fig. 2b. To isolate possible vibrations, a pneumatic isolation table was used to support the specimen and instrumentation. The table consists of a MDF open box frame, a construction foam core and aluminum top. MDF was chosen as a frame for its rigidity and lack of electrical conductivity and magnetic properties. The table is supported by four vertical pneumatic isolators (Newport Inc.). The optical components are clamped to the isolation table with highly damped material posts and post holders (Newport Inc.).

The experimental apparatus close-up photograph is introduced in Fig. 3. One can identify the ferromagnetic flapper attached to a glass rod holder by means of epoxy glue, located inside the activation zone of the AMFG. We focus here on flappers cut by means of spark erosion to cuboids of dimensions of



**Fig. 4.** The transverse displacement of the flapper as a function of the relative location along the flapper. A step like motion can be noticed, which resembles the qualitative shear motion presented in Fig. 1.

7(L) mm × 0.6(W) mm × 4(H) mm, and then electro-polished (MSM Krystall Inc.). The  $L$ - $W$  dimensions of the flapper are set to meet the  $H_1$ - $H_2$  plane of the AMFG. The displacement measurement of the flapper is based on capturing the shape changes using a 60 frames-per-second progressive scan CMOS camera (Jai® CV-A20 CL), and analyzed with an imaging software (Matrox™ Inspector 8.0). The displacements were first calculated relatively to a reference position of the specimen holder to eliminate the possible effect of rigid motions.

A typical transverse displacement of the flapper,  $u_y$ , as a function of the relative location along the flapper,  $x$ , is depicted in Fig. 4. This displacement is the difference between two extreme positions of the flapper. There are regions marked in the figure in which the local shear deformation  $\partial u_y / \partial x$  is about 5%, which is close to the maximal strain of this alloy [6]. Some other regions exhibit a negative deformation, perhaps due to switching with differently orientated variants. In other regions the local deformation is around zero. The average shear deformation  $\partial u_y / \partial x$  is about 0.6%. This value is larger by an order of magnitude than deformations obtained by piezoelectric actuation [3], but lower than the theoretical calculated values although the threshold field for variant rearrangement was reached [7]. An increase of the shear deformation by another order of magnitude is expected if a complete switching between the two relevant variants is obtained, either by increasing the magnetic

field amplitude, or by improving the specimen preparation. These measurements have demonstrated the use of  $Ni_2MnGa$  FSM flapper, which opens new frontiers in remote propulsion mechanisms. A more complete study of the motion of flappers in a fluidic media is underway, which include experimental measurements of thrust forces that are generated by this type of motion.

## References

- [1] R.J. Wood, The first takeoff of a biologically-inspired at-scale robotic insect, *IEEE Trans. Rob.* 24 (2008) 341–347.
- [2] R.J. Wood, S. Avadhanula, R. Sahai, E. Steltz, R.S. Fearing, Microrobot design using fiber reinforced composites, *J. Mech. Des.* 130 (2008) 5.
- [3] G. Kosa, M. Shoham, M. Zaaroor, Propulsion of a swimming micro medical robot, in: *Proceedings of the IEEE International Conference on Robotics and Automation ICRA 2005*, Barcelona, Spain, April 18–22, 2005, pp. 1327–1331.
- [4] P. Krulevitch, A.P. Lee, P.B. Ramsey, J.C. Trevino, J. Hamilton, M.A. Northrup, Thin film shape memory alloy microactuators, *J. MEMS* 5 (1996) 270–282.
- [5] K. Bhattacharya, R.V. Kohn, Symmetry texture and the recoverable strain of shape-memory polycrystals, *Acta Mater.* 44 (1996) 529–542.
- [6] R.D. James, M. Wuttig, Magnetostriction of martensite, *Philos. Mag. A* 77 (1998) 1273–1299.
- [7] Y. Ganor, D. Shilo, J. Messier, T.W. Shield, R.D. James, Testing system for ferromagnetic shape memory microactuators, *Rev. Sci. Instrum.* 78 (2007) 073907.
- [8] K. Bhattacharya, R.D. James, A theory of thin films of martensitic materials with applications to microstructures, *J. Mech. Phys. Solids* 47 (1999) 531–576.
- [9] R.D. James, Configurational forces in magnetism with application to the dynamics of a small-scale ferromagnetic shape memory cantilever, *Continuum Mech. Thermodyn.* 14 (2002) 55–86.
- [10] J. Kiang, L. Tong, Modeling of magneto-mechanical behavior of Ni–Mn–Ga single crystals, *J. Magn. Magn. Mater.* 292 (2005) 394–412.

Yaniv Ganor<sup>a,\*</sup>

Doron Shilo<sup>a</sup>

Nadege Zarrouati<sup>b</sup>

Richard D. James<sup>c</sup>

<sup>a</sup> Department of Mechanical Engineering, Israel Institute of Technology - Technion, Haifa 32000, Israel

<sup>b</sup> Department of Mechanics, Ecole Polytechnique, Palaiseau 91120, France

<sup>c</sup> Department of Aerospace Engineering and Mechanics, University of Minnesota, Minneapolis, MN 55455, USA

\* Corresponding author.

E-mail address: yanivg@tx.technion.ac.il

(Y. Ganor)

29 October 2008

Available online 6 January 2009